Nanoscale

COMMUNICATION

View Article Online
View Journal

Cite this: DOI: 10.1039/c6nr08088j

Received 14th October 2016,
Accepted 27th November 2016

DOI: 10.1039/c6nr08088j

www.rsc.org/nanoscale

Visible-light controlled catalytic Cu_2O–Au micromotors†

Dekai Zhou,‡[a,b] Yuguang C. Li,‡[a] Pengtao Xu,[a] Nicholas S. McCool,[a] Longqiu Li,*[b] Wei Wang[c] and Thomas E. Mallouk*[a]

Visible light driven Cu_2O–Au micromotors exhibit rapid on/off switching and speed control. Electrochemical measurements confirm that the light-induced movement of the Cu_2O–Au micromotors involves a self-electrophoresis mechanism modulated by the photoconductivity of Cu_2O. This study extends the utilization of the electromagnetic spectrum for micro/nanomotors into the visible range.

Autonomous micro/nanomotors are objects that can convert energy carried on board or supplied from their environment into mechanical motion. This idea was first demonstrated by Paxton *et al.*, who showed that platinum–gold nanorods could swim at speeds of several microns per second by decomposing hydrogen peroxide in aqueous solutions.[1] Since then, many different kinds of synthetic micro/nanomotors have been developed.[2–5] Different forms of input energy such as chemical,[1,6,7] magnetic,[8–12] electrical,[13,14] acoustic[15–23] and thermal[24,25] have been adapted to drive these motors. Gao and coworkers developed the first tubular micro-rockets that produced bubbles through an inner-surface-catalytic reaction to achieve self-propulsion in hydrogen peroxide solutions.[26] Wang and coworkers later demonstrated that asymmetrically shaped microrods could be induced to translate, rotate, align and assemble in response to ultrasonic standing waves in the MHz frequency range.[23] These fundamental studies have enabled a growing number of interesting motor functions and applications, such as drug or cargo delivery[11,16,17,27] and water remediation.[28–31] Wang and coworkers showed that metallic nanorods could be powered by resonant ultrasound to exhibit axial propulsion inside living Hela cells.[22] This capability was then adapted to the detection of trace biomolecules in cells *in vitro*.[32] Gao and coworkers have also used zinc-based micromotors in an *in vivo* mouse model to examine the distribution, retention, delivery of cargo, and the acute toxicity profile.[33]

Among the different propulsion mechanisms, light is one of the most interesting energy sources and has important prospects for applications that involve photo-activated and controlled micro/nanomotors. For example, Mou and Enachi demonstrated light-controlled bubble-propelled micromotors.[34,35] Esplandiu and Hong *et al.*, have developed two kinds of light-activated micropump systems with semiconductor materials.[36,37] Dong and coworkers demonstrated the efficient propulsion of UV light-driven TiO_2–Au Janus micromotors in aqueous solution.[38] Xuan and coworkers described fuel-free Janus mesoporous silica nanoparticle motors that were activated by near-infrared (NIR) laser light.[39] Palacci *et al.* realized self-organization of photoactivated colloidal particles.[40] Recently, Chen, Li and Dai proposed different methods for controlling the direction of motion of photo-activated micromotors.[41–43] For photo-driven micro/nanomotors, there are usually two major advantages: first, the speed of the micro/nanomotors can be controlled by the light intensity; secondly, light-driven micro/nano-motors can achieve rapid on/off control. Most of the photo-driven micro/nanomotors reported to date are activated either by UV or NIR light, which limits their utility, especially in environmental, sensing, and biomedical diagnostic applications. Here we describe a visible light-driven microscale Janus Cu_2O–Au micromotor that displays autonomous motion in low-concentration hydrogen peroxide solutions. By controlling the light intensity, the velocity of the Cu_2O–Au micromotors can be adjusted on demand, and the motion can be rapidly started or stopped by controlling the light source.

Cu_2O microparticles were synthesized by previously reported procedures (ESI†).[44] Fig. 1(a) shows the morphology of the Cu_2O particles, which are roughly spherical in shape with a diameter of about 1.2 μm. A 30 nm thick Au layer was evaporated onto the Cu_2O microparticles making half-covered

[a]*Departments of Chemistry, Biochemistry and Molecular Biology, and Physics, The Pennsylvania State University, University Park, PA 16802, USA. E-mail: tem5@psu.edu*

[b]*School of Mechatronics Engineering, Harbin Institute of Technology, Harbin 150001, China. E-mail: longqiuli@hit.edu.cn*

[c]*School of Materials Science and Engineering, Harbin Institute of Technology, Shenzhen Graduate School, Shenzhen, Guangdong 58055, China*

†Electronic supplementary information (ESI) available. See DOI: 10.1039/c6nr08088j

‡These authors contributed equally to this work.

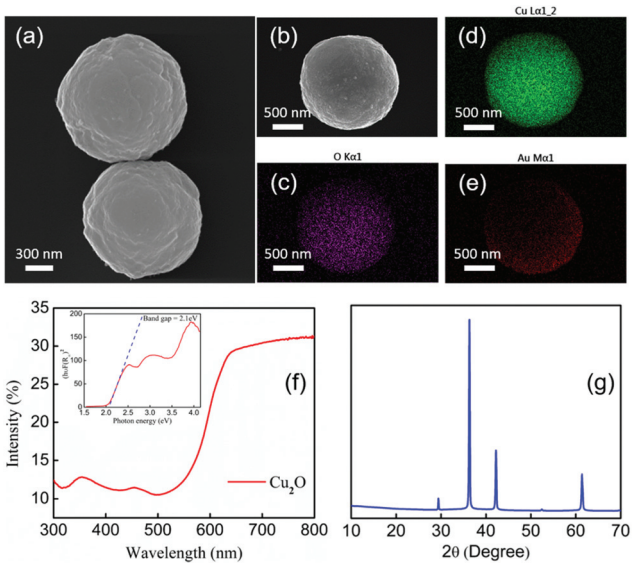

Fig. 1 Characterization of Cu_2O–Au microparticles: (a) SEM image of the as-synthesized Cu_2O particles. (b) SEM image of the Cu_2O–Au particles after Au coating. (c)–(e) EDS images of the Cu, Au and O elemental distribution on the Janus particles. (f) Diffuse-reflectance spectra of the Cu_2O particles confirming their visible light absorption. (g) XRD pattern of the Cu_2O particles.

Janus spheres, as shown in the SEM image in Fig. 1(b). Fig. 1(c), (d) and (e) show EDS mapping of the elemental composition of the Cu_2O–Au microparticles, which contain copper, gold and oxygen as expected from the synthesis. Copper and oxygen are evenly distributed whereas Au is concentrated on one side only.

Diffuse reflectance UV-visible spectra of the Cu_2O particles on glass substrates were measured to confirm their visible light absorption properties. Fig. 1(f) shows that the onset of absorption is at about 580 nm. A band gap of 2.1 eV was calculated from the Kubelka–Munk function by means of a Tauc plot,[45] which is shown in the inset of Fig. 2(f). The band gap of the Cu_2O particles is consistent with their previously reported semiconducting properties.[46,47] Fig. 2(g) shows X-ray diffraction patterns of the as-synthesized Cu_2O microparticles drop-cast onto a zero-background plate. Cu_2O was the major product with only a trace amount (<5%) of CuO detected by Rietveld refinement analysis.

Electrochemical experiments (Fig. 2) provided evidence that Cu_2O–Au micromotors are propelled by light-induced self-electrophoresis in H_2O_2 solutions (ESI†).[48] The generation and consumption of protons on the opposite sides of the Cu_2O–Au micromotors induces a proton concentration gradient, and the resulting electric field propels them with the Au side leading (see ESI, Video S-1†). When the Cu_2O microparticles are irradiated by visible light, the density of mobile electrons and holes increases, resulting in photoconduction and enhancement of the rate of the bipolar electrochemical decomposition of H_2O_2 at Cu_2O and Au. To confirm this mechanism of motility, Cu_2O microparticles without the gold coating were tested

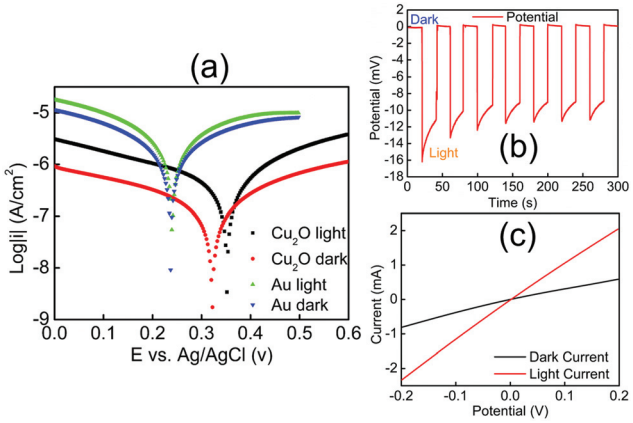

Fig. 2 Electrochemical characterizations of the Cu_2O–Au micromotors: (a) Tafel plots of the Au and Cu_2O on FTO electrodes measured against an Ag/AgCl reference under dark and light conditions in 2.5 v% H_2O_2. (b) *j*–*V* curve of a Cu_2O–Au solid junction electrode. (c) Light-chopping experiment with Cu_2O–Au solid junction electrode.

under the same conditions and only Brownian motion was observed under visible light (Video S-2†). A general consensus is that high salt concentrations decrease the velocity of self-electrophoretic micromotors either by increasing the conductivity of the double layer, or by inhibiting the reaction on the metal surface. Such effects are considered unique to electrophoretically driven particles, and are therefore popularly used to differentiate self-electrophoretis from diffusiophoresis.[49,50] In our experiments Cu_2O–Au micromotors exhibited only Brownian motion when illuminated in H_2O_2 solutions in the presence of 5 mM $NaNO_3$ (Video S-3†), which is again consistent with electrophoretic propulsion.

To better understand the mechanism of motility and effect of visible light, we measured the mixed potentials of Au and Cu_2O microelectrodes in 2.5 v% H_2O_2 solutions with and without illumination (ESI†). Fig. 2(a) shows Tafel plots for these electrodes. The mixed potential of the Au electrode is +0.24 V *vs.* Ag/AgCl in both the light and the dark, consistent with earlier measurements.[48] From the Tafel plot, the potential difference between Au and Cu_2O is about 80 mV in the dark. When illuminated, the Cu_2O electrode shifts in the positive

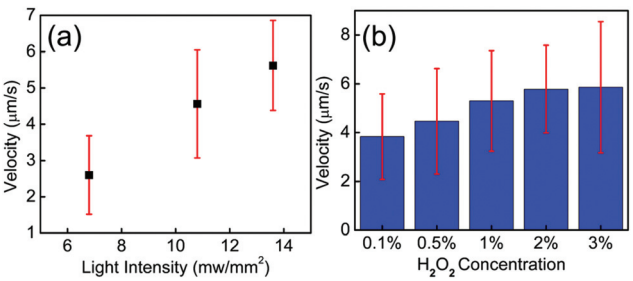

Fig. 3 (a) Speed of the Cu_2O–Au particles under different H_2O_2 concentrations. (b) Speed of the Cu_2O–Au particles under different light intensities, tested in 2.5 v% H_2O_2.

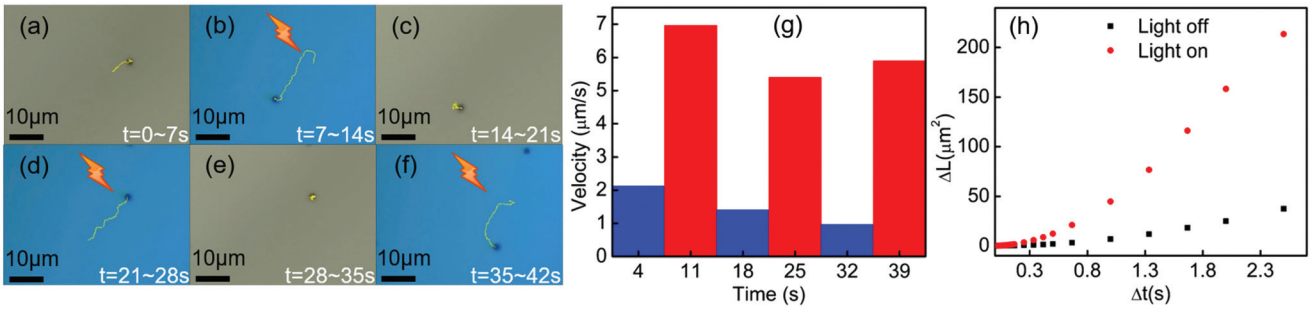

Fig. 4 (a)–(f) Time-lapse tracking line images of the Au–Cu_2O micromotors in 2.5 v% H_2O_2 with visible light and in the dark, taken every 7 s at a light intensity of 13.6 mW mm^{-2}. (g) Measured speed of the micromotors from the time lapse images (see Video S-4†). (h) Mean squared displacement of Au–Cu_2O micromotors with and without illumination (see Video S-4†), trajectories were showed on (a) and (b).

direction by about 30 mV, indicating a small photovoltage generated at the Cu_2O–solution interface. Because the potential of the Cu_2O electrode is positive relative to Au, electrons flow from Au to Cu_2O, and thus Au acts as the anode in the bipolar electrochemical decomposition of H_2O_2. This is consistent with the observation that Au is the leading end of the Cu_2O–Au micromotors. Fig. 2(b) shows the *j–V* curve of a Cu_2O–Au solid junction, where Cu_2O was electrodeposited onto a fluorine-doped tin oxide (FTO)-coated glass slide and Au was sputter-deposited onto the Cu_2O surface. The resistance of the Cu_2O–Au electrode decreased by a factor of about 3.5 under illumination, consistent with the photoconductivity of the insulating Cu_2O layer between the conductive FTO and Au layers. Fig. 2(c) shows a light-chopping experiment with the same Cu_2O–Au electrode, showing a photovoltage on the order of 10–15 mV. This is consistent with the shift in the mixed potential of Cu_2O observed in Fig. 2(a). Based on these data we can conclude that the dramatic increase in motility of Cu_2O–Au Janus particles arises from two effects, the photoconductivity of Cu_2O and the increase in the mixed potential difference under illumination.

To explore the parameters that control the mobility of the Cu_2O–Au micromotors, we examined the effects of H_2O_2 concentration and light intensity on motor velocity. Fig. 3(a) shows the velocity at different concentrations of H_2O_2. The speed of the Cu_2O–Au micromotors was close to 4 μm s^{-1} in 0.1 v% H_2O_2 and increased to 6 μm s^{-1} at 3 v% H_2O_2 concentration. As the concentration increased from 0.1 v% to 3 v%, we do not observe a proportional increase in the motor speed, suggesting that the conductivity of the Janus particle is rate-limiting. By changing neutral density (ND) filters, we varied the light intensity between 13.6 mW mm^{-2} and 5.8 mW mm^{-2}. From Fig. 3(b), we observe a linear relationship between motor speed and light intensity. This is consistent with the conclusion that the photoconductivity of the motors is rate-limiting. Fig. 4(a)–(f) illustrates the rapid on/off motion of the Cu_2O–Au micromotors. By tracking Video S-4,† the mean square displacement (MSD) of a Cu_2O–Au micromotor was calculated with and without illumination (Fig. S-2†). The ballistic speed of the Au–Cu_2O micromotors at short time scales was 6.9 μm s^{-1} under illumination, while the Brownian rotational time was found to be 2.3 seconds. A rather linear trajectory with a persistence length of ~16 μm is therefore expected. Without illumination, the MSD is linear indicating Brownian motion.[51] The highly repeatable and simple on/off motion control of the Cu_2O–Au micromotors under visible light may be useful in analytical applications where switching control is needed.

In conclusion, we have synthesized visible light-activated micromotors that can achieve rapid on/off control and variable speed by modulating the light intensity. The light-activated self-electrophoresis mechanism of the micromotors was confirmed by electrochemical methods. The utilization of visible light could enable the use of micro/nanomotors in analytical and environmental applications, as well as in fundamental studies of the interactions of powered particles.

Acknowledgements

This work was supported by the National Science Foundation under MRSEC grant number DMR- 1420620. W. Wang is grateful for the financial support from National Natural Science Foundation of China (Grant No. 11402069) and government of Shenzhen (Grant No. KQCX20140521144102503). D. Zhou, and L. Li, are grateful for the financial support from Nation Natural Science Foundation of China (51521003 and 51175129) and Program of Introducing Talents of Discipline to Universities (B07018) and Self-Planned Task of State Key Laboratory of Robotics and System (HIT) (SKLRS201607C).

Notes and references

1 W. F. Paxton, K. C. Kistler, C. C. Olmeda, A. Sen, St. S. K. Angelo, Y. Cao, T. E. Mallouk, P. E. Lammert and V. H. Crespi, *J. Am. Chem. Soc.*, 2004, **126**(41), 13424–13431.
2 W. Wang, W. Duan, S. Ahmed, T. E. Mallouk and A. Sen, *Nano Today*, 2013, **8**(5), 531–554.
3 W. Wang, W. Duan, S. Ahmed, A. Sen and T. E. Mallouk, *Acc. Chem. Res.*, 2015, **48**(7), 1938–1946.
4 K. K. Dey, F. Wong, A. Altemose and A. Sen, *Curr. Opin. Colloid Interface Sci.*, 2016, **21**, 4–13.

5 W. Gao and J. Wang, *ACS Nano*, 2014, **8**(4), 3170–3180.
6 M. Pumera, *Nanoscale*, 2010, **2**(9), 1643–1649.
7 S. Fournier-Bidoz, A. C. Arsenault, I. Manners and G. A. Ozin, *Chem. Commun.*, 2005, (4), 441–443.
8 R. Dreyfus, J. Baudry, M. L. Roper, M. Fermigier, H. A. Stone and J. Bibette, *Nature*, 2005, **437**(7060), 862–865.
9 A. Ghosh and P. Fischer, *Nano Lett.*, 2009, **9**(6), 2243–2245.
10 P. Fischer and A. Ghosh, *Nanoscale*, 2011, **3**(2), 557–563.
11 S. Tottori, L. Zhang, F. Qiu, K. K. Krawczyk, A. Franco-Obregón and B. J. Nelson, *Adv. Mater.*, 2012, **24**(6), 811–816.
12 T. Li, J. Li, H. Zhang, X. Chang, W. Song, Y. Hu, G. Shao, E. Sandraz, G. Zhang, L. Li and J. Wang, *Small*, 2016, **12**(44), 6098–6105.
13 P. Calvo-Marzal, S. Sattayasamitsathit, S. Balasubramanian, J. R. Windmiller, C. Dao and J. Wang, *Chem. Commun.*, 2010, **46**(10), 1623–1624.
14 S. T. Chang, V. N. Paunov, D. N. Petsev and O. D. Velev, *Nat. Mater.*, 2007, **6**(3), 235–240.
15 F. Nadal and E. Lauga, *Phys. Fluids*, 2014, **26**(8), 082001.
16 D. Kagan, M. J. Benchimol, J. C. Claussen, E. Chuluun-Erdene, S. Esener and J. Wang, *Angew. Chem., Int. Ed.*, 2012, **51**(30), 7519–7522.
17 S. Ahmed, W. Wang, L. O. Mair, R. D. Fraleigh, S. Li, L. A. Castro, M. Hoyos, T. J. Huang and T. E. Mallouk, *Langmuir*, 2013, **29**(52), 16113–16118.
18 V. Garcia-Gradilla, J. Orozco, S. Sattayasamitsathit, F. Soto, F. Kuralay, A. Pourazary, A. Katzenberg, W. Gao, Y. Shen and J. Wang, *ACS Nano*, 2013, **7**(10), 9232–9240.
19 S. Ahmed, D. T. Gentekos, C. A. Fink and T. E. Mallouk, *ACS Nano*, 2014, **8**(11), 11053–11060.
20 A. L. Balk, L. O. Mair, P. P. Mathai, P. N. Patrone, W. Wang, S. Ahmed, T. E. Mallouk, J. A. Liddle and S. M. Stavis, *ACS Nano*, 2014, **8**(8), 8300–8309.
21 V. Garcia-Gradilla, S. Sattayasamitsathit, F. Soto, F. Kuralay, C. Yardımcı, D. Wiitala, M. Galarnyk and J. Wang, *Small*, 2014, **10**(20), 4154–4159.
22 W. Wang, S. Li, L. Mair, S. Ahmed, T. J. Huang and T. E. Mallouk, *Angew. Chem.*, 2014, **126**(12), 3265–3268.
23 W. Wang, L. A. Castro, M. Hoyos and T. E. Mallouk, *ACS Nano*, 2012, **6**(7), 6122–6132.
24 H. R. Jiang, N. Yoshinaga and M. Sano, *Phys. Rev. Lett.*, 2010, **105**(26), 268302.
25 L. Baraban, R. Streubel, D. Makarov, L. Han, D. Karnaushenko, O. G. Schmidt and G. Cuniberti, *ACS Nano*, 2013, **7**(2), 1360–1367.
26 W. Gao, S. Sattayasamitsathit, J. Orozco and J. Wang, *J. Am. Chem. Soc.*, 2011, **133**(31), 11862–11864.
27 X. Ma, K. Hahn and S. Sanchez, *J. Am. Chem. Soc.*, 2015, **137**(15), 4976–4979.
28 L. Soler and S. Sanchez, *Nanoscale*, 2014, **6**(13), 7175–7182.
29 J. Orozco, V. García-Gradilla, M. D'Agostino, W. Gao, A. Cortés and J. Wang, *ACS Nano*, 2013, **7**(1), 818–824.
30 W. Gao, X. Feng, A. Pei, Y. Gu, J. Li and J. Wang, *Nanoscale*, 2013, **5**(11), 4696–4700.
31 M. Guix, J. Orozco, M. García, W. Gao, S. Sattayasamitsathit, A. Merkoçi, A. Escarpa and J. Wang, *ACS Nano*, 2012, **6**(5), 4445–4451.
32 B. Esteban-Fernández de Ávila, A. Martín, F. Soto, M. A. Lopez-Ramirez, S. Campuzano, G. M. Vásquez-Machado, W. Gao, L. Zhang and J. Wang, *ACS Nano*, 2015, **9**(7), 6756–6764.
33 W. Gao, R. Dong, S. Thamphiwatana, J. Li, W. Gao, L. Zhang and J. Wang, *ACS Nano*, 2015, **9**(1), 117–123.
34 F. Mou, Y. Li, C. Chen, W. Li, Y. Yin, H. Ma and J. Guan, *Small*, 2015, **11**(21), 2564–2570.
35 M. Enachi, M. Guix, V. Postolache, V. Ciobanu, V. M. Fomin, O. G. Schmidt and I. Tiginyanu, *Small*, 2016, **12**(39), 5497–5505.
36 M. J. Esplandiu, A. Farniya and A. Bachtold, *ACS Nano*, 2015, **9**(11), 11234–11240.
37 Y. Hong, M. Diaz, U. Cordova-Figueroa and A. Sen, *Adv. Func. Mater.*, 2010, **20**(10), 1568–1576.
38 R. Dong, Q. Zhang, W. Gao, A. Pei and B. Ren, *ACS Nano*, 2016, **10**(1), 839–844.
39 M. Xuan, Z. Wu, J. Shao, L. Dai, T. Si and Q. He, *J. Am. Chem. Soc.*, 2016, **138**(20), 6492–6497.
40 J. Palacci, S. Sacanna, A. P. Steinberg, D. J. Pine and P. M. Chaikin, *Science*, 2013, **339**(6122), 936–940.
41 W. Li, X. Wu, H. Qin, Z. Zhao and H. Liu, *Adv. Funct. Mater.*, 2016, **26**(18), 3164–3174.
42 C. Chen, F. Mou, L. Xu, S. Wang, J. Guan, Z. Feng, Q. Wang, L. Kong, W. Li, J. Wang and Q. Zhang, *Adv. Mater.*, 2016, DOI: 10.1002/adma.201603374.
43 B. Dai, J. Wang, Z. Xiong, X. Zhan, W. Dai, C.-C. Li, S.-P. Feng and J. Tang, *Nat. Nanotechnol.*, 2016, DOI: 10.1038/nnano.2016.187.
44 Z. Zhang, H. Che, J. Gao, Y. Wang, X. She, J. Sun, P. Gunawan, Z. Zhong and F. Su, *Catal. Sci. Technol.*, 2012, **2**(6), 1207–1212.
45 J. H. Nobbs, *Rev. Prog. Color. Relat. Top.*, 1985, **15**(1), 66–75.
46 M. Hara, T. Kondo, M. Komoda, S. Ikeda, J. N. Kondo, K. Domen, M. Hara, K. Shinohara and A. Tanaka, *Chem. Commun.*, 1998, (3), 357–358.
47 A. Paracchino, V. Laporte, K. Sivula, M. Grätzel and E. Thimsen, *Nat. Mater.*, 2011, **10**(6), 456–461.
48 Y. Wang, R. M. Hernandez, D. J. Bartlett, J. M. Bingham, T. R. Kline, A. Sen and T. E. Mallouk, *Langmuir*, 2006, **22**(25), 10451–10456.
49 S. Ebbens, D. A. Gregory, G. Dunderdale, J. R. Howse, Y. Ibrahim, T. B. Liverpool and R. Golestanian, *Europhys. Lett.*, 2014, **106**(5), 58003.
50 A. Brown and W. Poon, *Soft Matter*, 2014, **10**(22), 4016–4027.
51 W. Duan, M. Ibele, R. Liu and A. Sen, *Eur. Phys. J. E: Soft Matter Biol. Phys.*, 2012, **35**(8), 77.

